2017 IEEE 56th Annual Conference on Decision and Control (CDC)
December 12-15, 2017, Melbourne, Australia

Performance tradeoffs of dynamically controlled grid-connected inverters in low inertia power systems

Yan Jiang, Richard Pates, and Enrique Mallada

Abstract— **Implementing frequency response using grid-connected inverters is one of the popular proposed alternatives to mitigate the dynamic degradation experienced in low inertia power systems. However, such solution faces several challenges as inverters do not intrinsically possess the natural response to power fluctuations that synchronous generators have. Thus, to synthetically generate this response, inverters need to take frequency measurements, which are usually noisy, and subsequently make changes in the output power, which are therefore delayed. This paper explores the system-wide performance tradeoffs that arise when measurement noise, delayed actions, and power disturbances are considered in the design of dynamic controllers for grid-connected inverters. Using a recently proposed dynamic droop (iDroop) control for grid-connected inverters that is inspired by classical first order lead-lag compensation, we show that the sets of parameters that result in highest noise attenuation, power disturbance mitigation, and delay robustness do not necessarily have a common intersection. In particular, lead compensation is desired in systems where power disturbances are the predominant source of degradation, while lag compensation is a better alternative when the system is dominated by delays or frequency noise. Our analysis further shows that iDroop can outperform the standard droop alternative in both joint noise and disturbance mitigation, and delay robustness.**

I. Introduction

The composition of the electric gird is in state of flux [1]. Motivated by the need of reducing carbon emissions, conventional synchronous generators, with relatively large inertia, are being replaced with renewable energy sources with little (wind) or no inertia (solar) at all [2]. Alongside, neither the remaining generators, nor the demand, are compensating this loss. On the synchronous generator side, there are no incentives to provide additional frequency response beyond their natural one [3]. On the demand side, the steady increase of power electronics is gradually diminishing the load sensitivity to frequency variations [4]. As a result, rapid frequency fluctuations are becoming a major source of concern for several grid operators [5], [6]. Besides increasing the risk of frequency instabilities, this dynamic degradation also places limits on the total amount of renewable generation that can be sustained by the grid. Ireland, for instance, is already resourcing to wind curtailment –whenever wind becomes larger than 50% of existing demand– in order to preserve the grid stability.

This work was supported by NSF grants (CNS 1544771, EPCN 1711188), ARO contract W911NF-17-1-0092, and Johns Hopkins E^{2}SHI Seed Grant.

Yan Jiang and Enrique Mallada are with the Department of Electrical and Computer Engineering, Johns Hopkins University, Baltimore, MD 21218 USA (e-mails: {yjiang,mallada}@jhu.edu).

Richard Pates is with the Department of Automatic Control at Lund University, Lund, Sweden (e-mail: richard.pates@control.lth.se)

Among the several efforts under way to mitigate this dynamic degradation, one prominent alternative is to implement frequency response using (electronically coupled) inverter-based generation [7]. For example, in the US, the Federal Energy Regulatory Commission (FERC) has recently issued a notice of intent of rule making [8] that mandates frequency response by renewable generation. The goal is to use inverter-based generators to mimic synchronous generator behavior, or in other words, to implement virtual inertia [9]. However, while implementing virtual inertia can mitigate this degradation, it is unclear whether that particular choice of control is the most suitable for it. On the one hand, unlike generator dynamics that set the grid frequency, virtual inertia controllers estimate the grid frequency and its derivative using noisy and delayed measurements. On the other hand, inverter-based control can be significantly faster than conventional generators. Thus using inverters to mimic generators does not take advantage of their full potential.

Recently, a novel dynamic droop control (iDroop) [10] has been proposed as an alternative to virtual inertia. iDroop uses first order lead-lag compensation –inspired by scalable control laws in data networks [11]– and seeks to exploit the added flexibility present in inverters. Unlike virtual inertia that is sensitive to noisy measurements (it has unbounded H_2 norm [10]), iDroop experimentally improves the dynamic performance without the undesired unbounded noise amplification. In this paper we provide a theoretical foundation to such experimental findings. More precisely, for networks with homogeneous parameters, we analytically compute the dynamic performance (H_2 norm) of the control law proposed in [10] in the presence of both frequency measurements and power disturbances (Theorem 1). We show that iDroop not only is able to mitigate the noise amplification that virtual inertia introduces, but it can also outperform the standard droop control (Theorem 2). Furthermore, we analyze the robust stability of iDroop in the presence of delay and show that it can also outperform droop control (Theorem 3).

The analysis also unveils several intrinsic performance tradeoffs between power disturbances, measurement noise and delays, and how the lead-lag structure of iDroop is instrumental on the performance improvements. In particular, when the system is dominated by power disturbances, lead compensation provides the best performance. However, when the system is dominated by frequency noise, lag compensation is desired. Interestingly, the latter (lag compensation) matches the requirements for improving delay robustness with iDroop. However, achieving joint disturbance attenuation and delay robustness can be more challenging.

978-1-5090-2873-3/17/$31.00 ©2017 IEEE

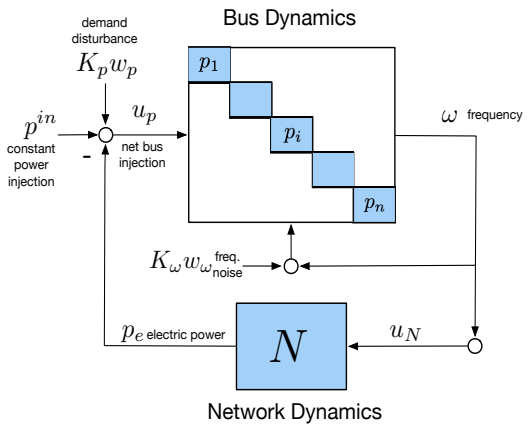

Fig. 1. Power Network Model

II. Preliminaries

A. Power Network Model

We use the power network model introduced in [12]. We consider a network of n buses denoted by $i \in V := \{1, \dots, n\}$. The power system dynamics are modeled as the feedback interconnection of bus dynamics $P := \text{diag}\,(p_i, i \in V)$ and network dynamics N as shown in Figure 1.

Bus Dynamics: Each subsystem p_i describes the ith bus dynamics where the input is the net bus power injection imbalance $u_{p,i}$ and the output is the frequency deviation from the nominal value ω_i. The bus dynamics of this paper are described in Figure 2 where g_i represents the generator dynamics and c_i the inverters dynamics. We assume that both dynamics are linear time invariant and thus

$$\hat{\omega}_i(s) = p_i(s)\hat{u}_{p,i}(s), \tag{1}$$

where $\hat{\omega}_i(s)$ and $\hat{u}_{p,i}(s)$ are the Laplace transform of $\omega_i(t)$ and $u_{p,i}(t)$, respectively.

The generator dynamics map the power injection $x_i(t) + u_{p,i}(t)$ to the bus frequency $\omega_i(t)$, and are represented in Laplace domain by

$$\hat{\omega}_i(s) = g_i(s)\left(\hat{x}_i(s) + \hat{u}_{p,i}(s)\right). \tag{2}$$

We use the swing dynamics to model g_i, i.e.,

$$g_i(s) = \frac{1}{M_i s + D_i} \tag{3}$$

where M_i is the aggregate generator's inertia and D_i is the aggregate generator's droop and frequency dependent load coefficient.

The inverter dynamics are modeled as

$$\hat{x}_i(s) = -c_i(s)\hat{\omega}_i(s) \tag{4}$$

where $\hat{x}_i(s)$ denotes the Laplace transform of $x_i(t)$ (the power injected by the inverter), and $c_i(s)$ represents the control law. Equation (4) assumes that inverters operate in frequency synchronized (grid-connected) mode [13], [14] where each inverter measures the local grid frequency $\omega_i(t)$ and statically sets the voltage phase of the inverter so that the output power is $x_i(t)$. This is a reasonable assumption as generator electro-mechanical dynamics are significantly slower than inverters.

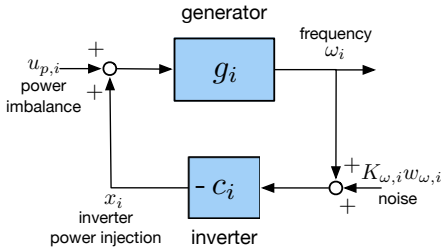

Fig. 2. Bus Dynamics p_i

We can use the control law $c_i(s)$ to model different algorithms that can be used to map $\omega_i(t)$ to $x_i(t)$. For example, $c_i(s) = R_{r,i}^{-1}$ and $c_i(s) = (\nu_i s + R_{r,i}^{-1})$, represent the standard droop and virtual inertia controllers, respectively. Similarly, the iDroop controller defined in [10] is given by

$$c_i(s) = \frac{\nu_i s + \delta_i R_{r,i}^{-1}}{s + \delta_i} \tag{5}$$

where $R_{r,i}^{-1}$ is the droop constant, and ν_i and δ_i are tunable parameters.

Combining (2) and (4) gives the input-output representation of the bus dynamics as

$$p_i(s) = \frac{1}{M_i s + D_i}\left(1 + \frac{c_i(s)}{M_i s + D_i}\right)^{-1}. \tag{6}$$

Network Dynamics: The network dynamics are given by

$$\hat{p}_e(s) = N(s)\hat{u}_N(s), \quad \text{where} \quad N(s) = \frac{1}{s}L_B, \tag{7}$$

$L_B \in \mathbb{R}^{n\times n}$ is the B_{ij}-weighted Laplacian matrix that describes how the transmission network couples the dynamics of different buses, i.e. $(L_B)_{ij}$ is equal to $-B_{ij}$, if $ij \in E$, $\sum_{e\in E} B_e$, if $i = j$, and 0 otherwise, where E is the set of lines.

State-Space Model: It will be useful to use the state space representation of the closed loop system of Figure 1. Using time domain versions of (2), (3), (4), and (7), the power system dynamics can be represented by

$$\dot{\theta} = \omega \tag{8a}$$

$$M\dot{\omega} = -D\omega - L_B\theta + x + p^{in} \tag{8b}$$

$$\dot{x} = -K_\delta(R_r^{-1}\omega + x) - K_\nu\dot{\omega} \tag{8c}$$

where $M := \text{diag}\,(M_i, i \in V)$, $R_r := \text{diag}\,(R_{r,i}, i \in V)$, $D := \text{diag}\,(D_i, i \in V)$, $K_\delta := \text{diag}\,(\delta_i, i \in V)$, $K_\nu := \text{diag}\,(\nu_i, i \in V)$, $\theta := (\theta_i, i \in V)$, $\omega := (\omega_i, i \in V)$, $x := (x_i, i \in V)$, and $p^{in} := (p_i^{in}, i \in V)$; we refer the reader to [12] for more details connecting the two models.

Equation (8) illustrates one of the potential challenges of implementing iDroop (or similarly virtual inertia), which comes from the need to measure $\dot{\omega}$ to implement (8c).

Fortunately, in the case of iDroop this can be avoided by considering the change of variable

$$x = z - K_\nu \omega. \tag{9}$$

Thus combining (8) with (9) gives

$$\dot{\theta} = \omega\,, \tag{10a}$$
$$M\dot{\omega} = -D\omega - L_B\theta + (z - K_\nu\omega) + p^{in}\,, \tag{10b}$$
$$\dot{z} = K_\delta(K_\nu - R_r^{-1})\omega - K_\delta z\,. \tag{10c}$$

To simplify our analysis we translate the equilibrium point of (10) to the origin. Since (10) is a linear time invariant system, this is equivalent to setting p^{in} to zero. Thus in the rest of this paper, we assume without loss of generality that $p^{in} = 0$.

B. Performance Measures

As mentioned before the aim of this paper is to evaluate how power disturbances, frequency measurement noise, and delay affect overall dynamic behavior, and in particular the frequency fluctuations, of the power network described in Figure 1. To this end we define specific performance metrics that will enable us to show that grid-connected inverters implementing iDroop can improve the performance beyond existing solutions.

Measurements Noise and Power Disturbances: We assume that the power system is being perturbed by two different signals (see figures 1 and 2): (i) $K_p w_p \in \mathbb{R}^n$, with $K_p = \operatorname{diag}(k_{p,i}, i \in V)$, that represents the fluctuations of the power injections at each bus; and (ii) $K_\omega w_\omega \in \mathbb{R}^n$, where $K_\omega = \operatorname{diag}(k_{\omega,i}, i \in V)$, that represents the frequency measurements noise that inverters experience at each bus. The signals w_p and w_ω represent uncorrelated stochastic white noise with zero mean and unit variance, i.e., $E[w_p(t)^T w_p(\tau)] = \delta(t-\tau)I_n$ and $E[w_\omega(t)^T w_\omega(\tau)] = \delta(t-\tau)I_n$.

Substituting ω with $\omega + K_\omega w_\omega$ on the RHS of (10b) and (10c), $p^{in} = 0$ with $K_p w_p$ in (10b), and defining $y = \omega$ as the output of (10) gives

$$\begin{bmatrix}\dot{\theta}\\ \dot{\omega}\\ \dot{z}\end{bmatrix} = A\begin{bmatrix}\theta\\ \omega\\ z\end{bmatrix} + B\begin{bmatrix}w_p\\ w_\omega\end{bmatrix}\,, \qquad y = C\begin{bmatrix}\theta\\ \omega\\ z\end{bmatrix}\,, \tag{11}$$

where

$$A = \begin{bmatrix} 0_{n\times n} & I_n & 0_{n\times n}\\ -M^{-1}L_B & -M^{-1}(D+K_\nu) & M^{-1}\\ 0_{n\times n} & K_\delta(K_\nu - R_r^{-1}) & -K_\delta\end{bmatrix}, \tag{12a}$$

$$B = \begin{bmatrix} 0_{n\times n} & 0_{n\times n}\\ M^{-1}K_p & -M^{-1}K_\nu K_\omega\\ 0_{n\times n} & K_\delta(K_\nu - R_r^{-1})K_\omega\end{bmatrix},\ C = \begin{bmatrix}0_{n\times n} & I_n & 0_{n\times n}\end{bmatrix}. \tag{12b}$$

Thus if we let G_{iDroop} denote the LTI system (11), we measure the effect of power disturbances and frequency measurements noise using the H_2 norm of G_{iDroop} which is given by

$$\|G_{\text{iDroop}}\|_{H_2}^2 = \lim_{t\to\infty} E[y^T(t)y(t)]. \tag{13}$$

The computation of the H_2 norm has been widely studied in control theory. In particular, one very useful procedure to compute $\|G_{\text{iDroop}}\|_{H_2}$ (see [15]) is based on

$$\|G_{\text{iDroop}}\|_{H_2}^2 = \operatorname{tr}(B^T X B) \tag{14}$$

where X is the observability Grammian, i.e. X solves the Lyapunov equation

$$A^T X + XA = -C^T C. \tag{15}$$

In the context of power systems this methodology has been first used in [16], where the authors seek to compute the power losses incurred by the network in the process of resynchronizing generators after a disturbance. Since then, several works have used similar metrics to evaluate effect of controllers on the power system performance, see e.g. [17], [18].

Delay Robustness: The frequency measurements available to the inverters will be subject to delay. When conducting inverter design, especially when considering inverters with fast dynamics and large gains, it is important to directly consider the effect of this delay to maintain the desired performance and prevent instability.

Delays to the frequency measurements can be easily accommodated into the models discussed in Section II-A by multiplying the inverter transfer fuction models $c_i(s)$ by $e^{-s\tau_i}$. For example, the iDroop contoller in (5) now becomes

$$c_i(s) = \frac{\nu_i s + \delta_i R_{r,i}^{-1}}{s + \delta_i} e^{-s\tau_i}.$$

Here the constant $\tau_i > 0$ corresponds to the delay to *i*th inverters frequency measurment. We then define the delay robustness τ_{rob} of power network model to be the largest $\tau > 0$ such that if

$$\tau_i < \tau,\ \forall i \in V,$$

then the model remains stable. The delay robustness therefore quanitifies how much delay to the frequency measurements can be tolerated before stability of the network is lost. This measure is in essence an adaptation of the phase margin to our power system network model, and provides a classical measure of robustness to assess the designed inverters.

III. Effect of Measurements Noise and Power Disturbances

In this section we evaluate how the relative intensity of the two type of stochastic disturbances (frequency measurement noise and power disturbances) affect the overall system performance using the H_2 norm metric $||G_{\text{iDroop}}||_{H_2}$ described in Section II-B. To make the analysis tractable, we assume homogeneous parameters $M_i = m$, $D_i = d$, $R_{r,i} = r_r$, $K_{p,i} = k_p$, $K_{\omega,i} = k_\omega$, $\delta_i = \delta$, and $\nu_i = \nu$, $\forall i \in V$.

In [10] it was shown that, if instead of iDroop, the inverters implement either Droop Control (DC) or virtual inertial (VI) then the H_2 norm is respectively given by

$$\|G_{\text{DC}}\|_{H_2}^2 = \frac{n[k_p^2 + (r_r^{-1}k_\omega)^2]}{2m(d + r_r^{-1})} \text{ and } \|G_{\text{VI}}\|_{H_2}^2 = +\infty, \tag{16}$$

where G_{DC} and G_{VI} represent the system (11) when the inverters implement droop control or virtual inertia respectively. In this section we compare (16) with the corresponding formulae for iDroop that is computed in Section III-A and show in Section III-B that iDroop can use its additional flexility to outperform DC and VI.

A. H_2-norm Performance of iDroop

We now compute the H_2 norm of iDroop. Since we assume homogeneous parameters we can decouple (11) into n subsystems. More precisely, let U be the orthonormal transformation that diagonalizes L_B. That is, $U^TU = UU^T = I_n$ such that $L_B = U\Gamma U^T$ where $\Gamma = \text{diag}\,(\lambda_1, \ldots, \lambda_n)$ with λ_i being the ith eigenvalue of L_B ordered in increasing order ($\lambda_1 = 0 \leq \lambda_2 \leq \cdots \leq \lambda_n$). Then, making the following change of variables $\theta = U\theta'$, $\omega = U\omega'$, $z = Uz'$, $y = Uy'$, $w_p = Uw'_p$, $w_\omega = Uw'_\omega$ leads to

$$\begin{bmatrix}\dot{\theta}'\\ \dot{\omega}'\\ \dot{z}'\end{bmatrix} = \begin{bmatrix}0_{n\times n} & I_n & 0_{n\times n}\\ -\frac{1}{m}\Gamma & -\frac{d+\nu}{m}I_n & \frac{1}{m}I_n\\ 0_{n\times n} & \delta(\nu - r_r^{-1})I_n & -\delta I_n\end{bmatrix}\begin{bmatrix}\theta'\\ \omega'\\ z'\end{bmatrix} + \begin{bmatrix}0_{n\times n} & 0_{n\times n}\\ \frac{k_p}{m}I_n & -\frac{\nu k_\omega}{m}I_n\\ 0_{n\times n} & \delta(\nu - r_r^{-1})k_\omega I_n\end{bmatrix}\begin{bmatrix}w'_p\\ w'_\omega\end{bmatrix}, \tag{17a}$$

$$y' = \begin{bmatrix}0_{n\times n} & I_n & 0_{n\times n}\end{bmatrix}\begin{bmatrix}\theta'\\ \omega'\\ z'\end{bmatrix}. \tag{17b}$$

Since (17) is composed by diagonal matrices, it is equivalent to n decoupled subsystems of the form

$$\begin{bmatrix}\dot{\theta}'_i\\ \dot{\omega}'_i\\ \dot{z}'_i\end{bmatrix} = A_i\begin{bmatrix}\theta'_i\\ \omega'_i\\ z'_i\end{bmatrix} + B_i\begin{bmatrix}w'_{p,i}\\ w'_{\omega,i}\end{bmatrix}, \quad y'_i = C_i\begin{bmatrix}\theta'_i\\ \omega'_i\\ z'_i\end{bmatrix}, \tag{18}$$

where

$$A_i = \begin{bmatrix}0 & 1 & 0\\ -\lambda_i/m & -(d+\nu)/m & 1/m\\ 0 & \delta(\nu - r_r^{-1}) & -\delta\end{bmatrix}, \tag{19a}$$

$$B_i = \begin{bmatrix}0 & 0\\ k_p/m & -\nu k_\omega/m\\ 0 & \delta(\nu - r_r^{-1})k_\omega\end{bmatrix},\ C_i = \begin{bmatrix}0 & 1 & 0\end{bmatrix}. \tag{19b}$$

Therefore, since U is an orthonormal transformation, it does not affect the H_2 norm of (11), and it will allow us to compute the H_2 norm of (11) by making n simpler H_2 norm computations using (18).

Theorem 1 (H_2 norm of iDroop): The H_2 norm of the system (11), i.e. $||G_{\text{iDroop}}||_{H_2}$ is given by

$$\|G_{\text{iDroop}}\|^2_{H_2} = \frac{n(k_p^2 + \nu^2 k_\omega^2)}{2m(d+\nu)} + \sum_{i=1}^{n}\frac{\delta^2(\nu - r_r^{-1})\left[\dfrac{k_p^2 + \nu^2 k_\omega^2}{d+\nu} - (\nu + r_r^{-1})k_\omega^2\right]}{2\left[(d+\nu+m\delta)\delta(d+r_r^{-1}) + (d+\nu)\lambda_i\right]}. \tag{20}$$

In some cases, it will be convenient to make explicit the dependence of the H_2 norm of iDroop on the parameters ν and δ. Thus we will also use $\|G_{\text{iDroop}}\|^2_{H_2}(\nu, \delta)$ to refer to (20). The entire proof of this theorem is omitted due to space constraints and can be found in [19]. We provide a proof sketch below.

Proof: We compute $||G_{\text{iDroop}}||_{H_2}$ by computing instead the norm of n orthogonal subsystems $G_{\text{iDroop},i}$ described by (18), i.e., $||G_{\text{iDroop},i}||_{H_2}$. Then, the total system norm can be computed using: $||G_{\text{iDroop}}||^2_{H_2} = \sum_{i=1}^{n}||G_{\text{iDroop},i}||^2_{H_2}$.

Therefore we need to solve the Lyapunov equation

$$A_i^TQ + QA_i = -C_i^TC_i, \tag{21}$$

where A_i is given by (19a) and Q must be symmetric.

Whenever $\lambda_i \neq 0$ (21) has a unique solution for Q. Thus, solving for Q in (21) gives

$$\|G_{\text{iDroop},i}\|^2_{H_2} = \text{tr}(B_i^TQB_i) = \frac{k_p^2 + \nu^2k_\omega^2}{2m(d+\nu)} + \frac{\delta^2(\nu - r_r^{-1})\left[\dfrac{k_p^2 + \nu^2k_\omega^2}{d+\nu} - (\nu + r_r^{-1})k_\omega^2\right]}{2\left[(d+\nu+m\delta)\delta(d+r_r^{-1}) + (d+\nu)\lambda_i\right]}. \tag{22}$$

When $\lambda_i = 0$, i.e., $i = 1$, neither $\dot{\omega}'_1$, nor $\dot{z}'_1$, nor y'_1 depend on θ'_1 in (18). Thus θ'_i is not observable and we can simplify the subsystem described by (18) to

$$\begin{bmatrix}\dot{\omega}'_1\\ \dot{z}'_1\end{bmatrix} = \tilde{A}_1\begin{bmatrix}\omega'_1\\ z'_1\end{bmatrix} + \tilde{B}_1\begin{bmatrix}w'_{p,1}\\ w'_{\omega,1}\end{bmatrix}, \quad y'_1 = \tilde{C}_1\begin{bmatrix}\omega'_1\\ z'_1\end{bmatrix}, \tag{23}$$

where, for the simplified subsystem, we have

$$\tilde{A}_1 = \begin{bmatrix}-(d+\nu)/m & 1/m\\ \delta(\nu - r_r^{-1}) & -\delta\end{bmatrix}, \tag{24a}$$

$$\tilde{B}_1 = \begin{bmatrix}k_p/m & -\nu k_\omega/m\\ 0 & \delta(\nu - r_r^{-1})k_\omega\end{bmatrix}, \quad \tilde{C}_1 = \begin{bmatrix}1 & 0\end{bmatrix}. \tag{24b}$$

Thus a similar computation as for the case $\lambda_i \neq 0$ shows that $\|G_{\text{iDroop},1}\|^2_{H_2}$ is also defined by (22) with $\lambda_i = 0$. Result follows. ∎

B. iDroop Performance Improvement

We now show using Theorem 1 that iDroop can adapt to different network conditions and improve the system performance. Since virtual inertia has infinite H_2 norm (c.f. (16)), we compare here the performance of iDroop, i.e., $\|G_{\text{iDroop}}\|_{H_2}$, with inverters implementing standard droop control, i.e., $\|G_{\text{DC}}\|_{H_2}$. We achieve this goal by finding the set of parameter values ν and δ that minimizes (20) and showing that for such values $\|G_{\text{iDroop}}\|_{H_2} \leq \|G_{\text{DC}}\|_{H_2}$. The following auxiliary lemmas help us pave the way to the main result of this section (Theorem 2).

Lemma 1: If $\delta \to +\infty$, then $\|G_{\text{iDroop}}\|^2_{H_2} = \|G_{\text{DC}}\|^2_{H_2}$.

Proof: When $\delta \to +\infty$, (22) can be reduced as

$$\begin{aligned}
&\lim_{\delta\to+\infty} \|G_{\text{iDroop},i}\|_{H_2}^2 \\
&= \frac{k_p^2+\nu^2k_\omega^2}{2m(d+\nu)} + \frac{(\nu-r_r^{-1})\{k_p^2-\left[\nu d+r_r^{-1}(d+\nu)\right]k_\omega^2\}}{2m(d+\nu)(d+r_r^{-1})} \\
&= \frac{k_p^2}{2m(d+r_r^{-1})} + \frac{\left[\nu r_r^{-1}(d+r_r^{-1})-(\nu-r_r^{-1})r_r^{-1}d\right]k_\omega^2}{2m(d+\nu)(d+r_r^{-1})} \\
&= \frac{k_p^2}{2m(d+r_r^{-1})} + \frac{\left(\nu r_r^{-2}+r_r^{-2}d\right)k_\omega^2}{2m(d+\nu)(d+r_r^{-1})} \\
&= \frac{k_p^2+\left(r_r^{-1}k_\omega\right)^2}{2m(d+r_r^{-1})} =: \|G_{\text{DC},i}\|_{H_2}^2 \,, \qquad (25)
\end{aligned}$$

where $\|G_{\text{DC},i}\|_{H_2}$ denotes the H_2 norm of the ith subsystem (18) when droop control with gain r_r is used instead of iDroop. Thus it follows that $\|G_{\text{DC}}\|_{H_2}^2 = \sum_{i=1}^n \|G_{\text{DC},i}\|_{H_2}^2$ which gives (16). ∎

Thus we have shown that as $\delta \to +\infty$ $\|G_{\text{iDroop}}\|_{H_2}$ asymptotically converges to $\|G_{\text{DC}}\|_{H_2}$. Our second lemma will show that this convergence is monotonically from either above or below depending on the value of ν. For a given ν, we use $f(\delta)$ to denote the dependence of $\|G_{\text{iDroop}}\|_{H_2}^2$ with respect to δ, i.e.

$$f(\delta) = \sum_{i=1}^n f_i(\delta) = n\alpha_5 + \sum_{i=1}^n \frac{\alpha_1\delta^2}{\alpha_2\delta^2+\alpha_3\delta+\alpha_4(\lambda_i)} \qquad (26)$$

with

$$\alpha_1 = (\nu-r_r^{-1})\left[\frac{k_p^2+\nu^2k_\omega^2}{d+\nu} - (\nu+r_r^{-1})k_\omega^2\right] \,, \quad (27a)$$

$$\alpha_2 = 2m(d+r_r^{-1}) \,,\ \alpha_3 = 2(d+\nu)(d+r_r^{-1}) \,, \quad (27b)$$

$$\alpha_4(\lambda_i) = 2(d+\nu)\lambda_i \,, \qquad \alpha_5 = \frac{k_p^2+\nu^2k_\omega^2}{2m(d+\nu)} \,. \quad (27c)$$

Lemma 2: For any positive δ, $f(\delta)$ is a monotonically increasing or decreasing function if and only if α_1 is positive or negative, respectively. That is, $\text{sign}\left(f'(\delta)\right) = \text{sign}\left(\alpha_1\right)$.

Proof: Using (26) we compute the derivative of $f(\delta)$ which gives

$$f'(\delta) = \sum_{i=1}^n \alpha_1 \frac{\alpha_3\delta^2+2\alpha_4(\lambda_i)\delta}{(\alpha_2\delta^2+\alpha_3\delta+\alpha_4(\lambda_i))^2}$$

From (27), we can easily see that α_2 and α_3 are positive since $m > 0$, $d > 0$, $\nu > 0$, and $r_r > 0$. Also, given that all the eigenvalues of the Laplacian matrix L_B are nonnegative, $\alpha_4(\lambda_i)$ must be nonnegative. Thus, $\forall\delta > 0$, $(\alpha_3\delta^2+2\alpha_4(\lambda_i)\delta)/(\alpha_2\delta^2+\alpha_3\delta+\alpha_4(\lambda_i))^2 > 0$. So the sign of $f'(\delta)$ is determined by α_1 for any $\delta > 0$. ∎

Lemmas 1 and 2 suggest that in order to improve performance one needs to set ν such that $\alpha_1 > 0$ and δ as small as practically possible. The last lemma characterizes the optimal ν^* that minimizes the H_2 norm of iDroop when $\delta = 0$.

Lemma 3: Let

$$g(\nu) := \|G_{\text{iDroop}}\|_{H_2}^2(\nu,0) = \frac{n(k_p^2+\nu^2k_\omega^2)}{2m(d+\nu)} \qquad (28)$$

be the value of the H_2 norm of iDroop when $\delta = 0$. Then, within the domain of interest $\nu \geq 0$, $g(\nu)$ is minimized by

$$\nu^* = -d + \sqrt{d^2+k_p^2/k_\omega^2}. \qquad (29)$$

Proof: We take the derivate of (28) with respect to ν which gives

$$g'(\nu) = \frac{k_\omega^2\nu^2+2k_\omega^2d\nu-k_p^2}{2m(d+\nu)^2} \,. \qquad (30)$$

By equating (30) to 0, we can solve the corresponding ν as $\nu_\pm^* = -d \pm \sqrt{d^2+k_p^2/k_\omega^2}$. The only positive root is therefore $\nu^* = -d + \sqrt{d^2+k_p^2/k_\omega^2}$. Since the denominator of (30) is always positive and the highest order coefficient of the numerator is positive, whenever $0 < \nu < \nu^*$, then $g'(\nu) < 0$, and if $\nu > \nu^*$, then $g'(\nu) > 0$. Therefore, ν^* is actually the minimizer of $g(\nu)$ and $g(\nu^*)$ is the minimum. ∎

We are now ready to prove the main result of this section.

Theorem 2: Let $\|G_{\text{iDroop}}\|_{H_2}^2(\nu,\delta)$ be the (ν,δ)-dependent H_2 norm of iDroop given in (20). Let ν^* be as defined in (29). Then, whenever $\left(k_p/k_\omega\right)^2 \neq 2r_r^{-1}d + r_r^{-2}$, setting

$$\nu \in [\nu^*, r_r^{-1}) \quad \text{or} \quad \nu \in (r_r^{-1}, \nu^*], \qquad (31)$$

gives $\|G_{\text{iDroop}}\|_{H_2}^2(\nu,\delta) < \|G_{\text{DC}}\|_{H_2}^2$ for all $\delta \geq 0$. Moreover, $\|G_{\text{iDroop}}\|_{H_2}^2(\nu^*,0)$ provides the global minimum H_2 norm. When $\left(k_p/k_\omega\right)^2 = 2r_r^{-1}d + r_r^{-2}$, then $\|G_{\text{iDroop}}\|_{H_2}^2(\nu^* = r_r^{-1},\delta) = \|G_{\text{DC}}\|_{H_2}^2$.

Proof: By Lemma 2, for a given ν, if $\alpha_1 < 0$, then $f'(\delta) < 0$, which follows that $\|G_{\text{iDroop}}\|_{H_2}^2$ always decreases as δ increases. However, according to Lemma 1, even if $\delta \to \infty$, we can only obtain $\|G_{\text{iDroop}}\|_{H_2}^2 = \|G_{\text{DC}}\|_{H_2}^2$. Similarly, if $\alpha_1 = 0$, then $f'(\delta) = 0$, which indicates that $\|G_{\text{iDroop}}\|_{H_2}^2$ keeps constant as δ increases, so no matter what the value of δ we use, we will always obtain $\|G_{\text{iDroop}}\|_{H_2}^2 = \|G_{\text{DC}}\|_{H_2}^2$. Therefore, iDroop control cannot outperform DC when $\alpha_1 \leq 0$. Thus we constrain to $\alpha_1 > 0$ from now on. In this case, $f'(\delta) > 0$, which shows that $\|G_{\text{iDroop}}\|_{H_2}^2$ always increases as δ increases, so choosing δ arbitrarily small is optimal for fix ν.

We now look at the values of ν that satisfy the requirement $\alpha_1 > 0$. α_1 can be rearranged as follows:

$$\alpha_1 = \frac{\beta_2\nu^2+\beta_1\nu+\beta_0}{d+\nu} \,,$$

where $\beta_2 = -k_\omega^2(d+r_r^{-1})$, $\beta_1 = (k_p^2+k_\omega^2r_r^{-2})$, and $\beta_0 = -r_r^{-1}(k_p^2-k_\omega^2r_r^{-1}d)$. Since the denominator of α_1 is always positive, the sign of α_1 is only decided by its numerator. Let $N_{\alpha_1}(\nu)$ be the numerator of α_1. Thus, $N_{\alpha_1}(\nu)$ is a univariate quadratic function in ν, whose roots are:

$$\nu_1 = r_r^{-1} \,, \quad \text{and} \quad \nu_2 = \frac{\left(k_p/k_\omega\right)^2 - r_r^{-1}d}{d+r_r^{-1}} \,.$$

Since $\beta_2 < 0$, the graph of $N_{\alpha_1}(\nu)$ is a parabola that opens downwards. Therefore, if $\nu_1 < \nu_2$, then $\nu \in (\nu_1,\nu_2)$ guarantees $\alpha_1 > 0$; if $\nu_1 > \nu_2$, then $\nu \in (\nu_2,\nu_1) \cap [0,\infty)$ guarantees $\alpha_1 > 0$. Notably, if $\nu_1 = \nu_2$, there exists no feasible points of ν to make $\alpha_1 > 0$. This can only happen

if $(k_p/k_\omega)^2 = 2r_r^{-1}d + r_r^{-2}$, and in this case $\nu_1 = \nu^* = \nu_2 = r_r^{-1}$ and therefore iDroop can only match the performance of DC by setting $\nu = r_r^{-1}$ and choosing any $\delta \geq 0$, i.e., $\|G_{\text{iDroop}}\|_{H_2}^2(\nu^* = r_r^{-1}, \delta) = \|G_{\text{DC}}\|_{H_2}^2$. This shows the last statement of the theorem.

We now focus in the case where the set

$$S = (\nu_1, \nu_2) \cup \{(\nu_2, \nu_1) \cap [0, \infty)\}$$

is nonempty. Thus, for any fix $\nu \in S$, $\alpha_1 > 0$, and thus by Lemma 2 setting $\delta = 0$ achieves the minimum norm, i.e. $\|G_{\text{iDroop}}\|_{H_2}^2(\nu, 0) < \|G_{\text{iDroop}}\|_{H_2}^2(\nu, \delta)\ \forall \delta > 0$. Since by Lemma 3, ν^* is the minimizer of $g(\nu) = \|G_{\text{iDroop}}\|_{H_2}^2(\nu, 0)$, as long as $\nu^* \in S$, $(\nu^*, 0)$ globally minimizes $\|G_{\text{iDroop}}\|_{H_2}^2(\nu, \delta)$. In fact, we will show next that ν^* is always within S whenever $S \neq \emptyset$.

First we consider the situation where $\nu_1 < \nu_2$, which implies that $(k_p/k_\omega)^2 > 2r_r^{-1}d + r_r^{-2}$. Then we have

$$\begin{aligned}\nu^* &= -d + \sqrt{d^2 + k_p^2/k_\omega^2} > -d + \sqrt{d^2 + 2r_r^{-1}d + r_r^{-2}} \\ &= -d + \sqrt{(d + r_r^{-1})^2} = r_r^{-1} = \nu_1\ .\end{aligned}$$

We also want to show that $\nu^* < \nu_2$ which holds iff $\sqrt{d^2 + k_p^2/k_\omega^2} < \dfrac{(k_p/k_\omega)^2 - r_r^{-1}d}{d + r_r^{-1}} + d = \dfrac{(k_p/k_\omega)^2 + d^2}{d + r_r^{-1}}$ $\iff$ $1 < \dfrac{\sqrt{d^2 + k_p^2/k_\omega^2}}{d + r_r^{-1}}$, which always holds since $(k_p/k_\omega)^2 > 2r_r^{-1}d + r_r^{-2}$. Thus, $\nu_1 < \nu^* < \nu_2$. Similarly, we can prove that in the situation where $\nu_1 > \nu_2$, $\nu_2 < \nu^* < \nu_1$ holds and thus $\nu^* \in (\nu_2, \nu_1) \cap [0, \infty)$. Thus, it follows that $(\nu^*, 0)$ is the global minimizer of $\|G_{\text{iDroop}}\|_{H_2}^{2*}(\nu, \delta)$.

Finally, from (16) and (20), it is easy to see that $\|G_{\text{DC}}\|_{H_2}^2 = \|G_{\text{iDroop}}\|_{H_2}^2(r_r^{-1}, 0)$. From the proof of Lemma 3 it follows that when $\nu < \nu^*$ (resp. $\nu > \nu^*$) then $\|G_{\text{iDroop}}\|_{H_2}^2(\nu, 0) = g(\nu)$ decreases (resp. increases) monotonically. Therefore, whenever ν satisfies (31) we have

$$\|G_{\text{DC}}\|_{H_2}^2 = \|G_{\text{iDroop}}\|_{H_2}^2(r_r^{-1}, 0) > \|G_{\text{iDroop}}\|_{H_2}^2(\nu, 0).$$

Result follows. ∎

Theorem 2 shows that in order to optimally improve the performance iDroop needs to first set δ arbitrarily close to zero. Interestingly, this implies that the the transfer function $c_i(s) \simeq \nu$ except for $c_i(0) = r_r^{-1}$. In other words, iDroop uses its first order lead/lag property to effectively decouple the zero-frequency gain $c_i(0)$ from all the other frequencies $c_i(j\omega_0) = \simeq \nu$. This decouple is particularly easy to understand in two special regimes: (i) If $k_p \ll k_\omega$, the system is dominated by frequency measurements and therefore $\nu^* \simeq 0$. In this case, we have $0 \simeq \nu^* < r_r^{-1}$ which makes iDroop a lag compensator. Thus, by using lag compensation (setting $\nu < r_r^{-1}$) iDroop can attenuate frequency noise; (ii) If $k_p \gg k_\omega$, the system is dominated by power disturbances and $\nu^* \simeq k_p/k_\omega \gg 1$. Thus, for k_p/k_ω large enough, $\nu^* > r_r^{-1}$ and thus iDroop can use lead compensation (setting $\nu > r_r^{-1}$) to help mitigate power disturbances.

IV. Delay Robustness

A. Stability under Delays

As discussed in Section II-B, calculating the delay robustness amounts to computing the largest delays τ_i that maintain stability of the network model. In the heterogeneous inverter setting this can be addressed in a decentralized manner using Theorem 3.2 from [12]. To give simpler and more interpretable formulae that can be directly compared with those for H_2 performance, here we instead consider the homogeneous parameter setting. In this case stability criteria for any inverter design can be obtained directly from the multivariable Nyquist criterion of [20].

Corollary 1 ([20]): Assuming homogeneous parameters and that $c(s)$ is stable, the network model is stable if and only if

$$\sum_{i=1}^{n} \text{w.n.o.} \frac{sc(s)\, e^{-s\tau}}{ms^2 + ds + \lambda_i} = 0.$$

In the above w.n.o. denotes the winding number about the -1 point of the given transfer functions as evaluated on the usual Nyquist contour.

Proof: First observe that $P(s) = \bar{P}(s)\left(I_n + C\bar{P}(s)\right)^{-1}$, where $\bar{P} = \frac{1}{ms+d} I$ and $C(s) = c(s)\, I$. Therefore the network model is equivalent to $\bar{P}(s)$ in negative feedback with $\frac{1}{s} L_B$ and $C(s)$. By closing the network feedback loop, it then follows that the model is stable if and only if the negative feedback interconnection of $\bar{P}(s)\left(I_n + \frac{1}{s} L_B \bar{P}(s)\right)^{-1}$ and $C(s)$ is stable. Provided $d > 0$, it is easily shown that $\bar{P}(s)\left(I_n + \frac{1}{s} L_B \bar{P}(s)\right)^{-1}$ is stable (using e.g. a passivity argument), and so by the multivariable Nyquist criterion, the network model is stable if and only if

$$\text{w.n.o. } \lambda\left(C(s)\,\bar{P}(s)\left(I_n + \frac{1}{s} L_B \bar{P}(s)\right)^{-1}\right) = 0.$$

In the above w.n.o. $\lambda(\cdot)$ denotes the winding number of the eigenloci of the given matrix, evaluated on the usual Nyquist contour; see [20] for details. Since $C(s), \bar{P}(s)$ and L_B are all normal, commuting matrices, the eigenvalues of $C(s)\,\bar{P}(s)\left(I_n + \frac{1}{s} L_B \bar{P}(s)\right)^{-1}$ are easily shown to be

$$\frac{sc(s)\, e^{-s\tau}}{ms^2 + ds + \lambda_i},$$

from which the result follows immediately. ∎

B. Delay Robustness of iDroop

Corollary 1 shows that in order to calculate the delay robustness, we need to calculate the largest τ such that a winding number condition is satsfied. This is straightforward to do numerically, however to facilitate comparison with H_2 performance analysis, we will explicitly compute the delay robustness when the iDroop controller is used in the two extreme regimes $\delta = 0$ and $\delta \to \infty$.

Theorem 3 (Delay Robustness of iDroop): Define

$$\omega_n(x) = \sqrt{\sqrt{x^2 + \frac{2x\lambda_n}{m}} + x + \frac{\lambda_n}{m}}.$$

Assuming homogeneous parameters, then:

(i) If $\delta = 0$ and $d < \nu$, iDroop's delay robustness equals

$$\tau_{\text{rob}} = \frac{1}{\omega_n\left(\frac{1}{2m^2}\left(\nu^2 - d^2\right)\right)} \arccos\left(-\frac{d}{\nu}\right).$$

(ii) If $\delta \to \infty$ and $d < r_r^{-1}$, then

$$\tau_{\text{rob}} = \frac{1}{\omega_n\left(\frac{1}{2m^2}\left(r_r^{-2} - d^2\right)\right)} \arccos\left(-\frac{d}{r_r^{-1}}\right).$$

Proof: Observe that in both limiting cases,

$$c\left(j\omega\right) \to a, \forall \omega \in \mathbb{R},$$

where $a > 0$ (for $\delta = 0$, $a = \nu$, and for $\delta \to \infty$, $a = r_r^{-1}$). Therefore to prove the result, by Corollary 1, we need a method to calculate the winding numbers of the transfer functions

$$\frac{sae^{-s\tau}}{ms^2 + ds + \lambda_i}. \tag{33}$$

Observe that if $\tau \equiv 0$, then the Nyquist diagrams for all these transfer functions are circles that cut the real axis at the origin and $\frac{a}{d}$. This implies that the phase margin ϕ for all these transfer functions are the same, and the winding number condition is satsified if and only if

$$\max_{i \in V} \omega_i \tau < \phi.$$

In the above, ω_i is the largest frequency at which the ith transfer function has magnitude one (the frequency used to calculate the phase margin). A simple calculation shows that

$$\cos\left(\pi - \phi\right) = \frac{d}{a}.$$

To complete the proof we then only need to find the frequencies ω_i; that is solve the equation

$$\left|j\omega a\right| = \left|-m\omega^2 + dj\omega + \lambda_i\right|.$$

This can be done by solving a fourth order polynomial equation. The general solution is given by

$$\omega_i = \sqrt{\sqrt{x^2 + \frac{2x\lambda_i}{m}} + x + \frac{\lambda_i}{m}},$$

where $x = \frac{1}{2m^2}\left(a^2 - d^2\right)$. Since the above is monotonically inreasing in λ_i, the result follows. ∎

Although the above precisely gives τ_{rob} for iDroop in terms of the network parameters, it is a little hard to interpret. However if we assume that $d = 0$, and replace $\omega_n\left(x\right)$ with the upper bound

$$\omega_n\left(x\right) \leq \sqrt{2}\sqrt{x + \frac{m}{\lambda_n}},$$

we get the following much simplified lower bound for τ_{rob}:

$$\tau_{\text{rob}} \geq \frac{m\pi}{2\sqrt{a^2 + 2m\lambda_n}}.$$

In the above $a = \nu$ when $\delta = 0$, and $a = r_r^{-1}$ when $\delta \to \infty$. We therefore clearly see that the delay robustness may be improved using iDroop by setting ν small, though this should be balanced with the desired objectives in the H_2 norm. In particular, in systems where power disturbances dominates over frequency noise, jointly improving H_2 and delay robustness may be not possible.

Remark 1: In the case that $\nu \leq d$ or $r_r^{-1} \leq d$ (that is when we are outside the scope of Theorem 3), the delay robusntess of iDroop is arbitrarily large. In such a regime, iDroop is stable when subject to delays of any size.

V. Numerical Illustrations

In this section we present simulation results that compare iDroop to standard droop control. We show that setting iDroop parameters as suggested in this paper improves performance if the system is subject to power disturbances, measurement noise, and delay.

The simulations are conducted on the IEEE 39 bus system (New England) available with the Power System Toolbox [21]. Since the system parameters in this model violate our homogeneity assumption, for the purposes of iDroop design, we take the inertia m equal to the average of the inertia in the dataset, i.e., $m = 0.02$. Since the load frequency coefficient is not present, we set in our simulations $D_i = 0.267$ at every bus and therefore $d = 0.267$. The simulations are still conducted with the heterogeneous parameters. We further add an inverter to ever generator bus. The droop coefficient of each inverter is then set for both iDroop and droop control to $R_{r,i} = r_r = 0.5$.

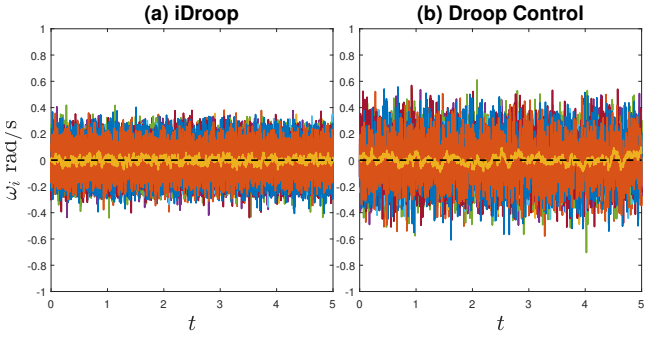

Fig. 3. Frequency deviations of the system when power disturbances and measurements noise are introduced with $k_p = 1.5$ and $k_\omega = 0.15$

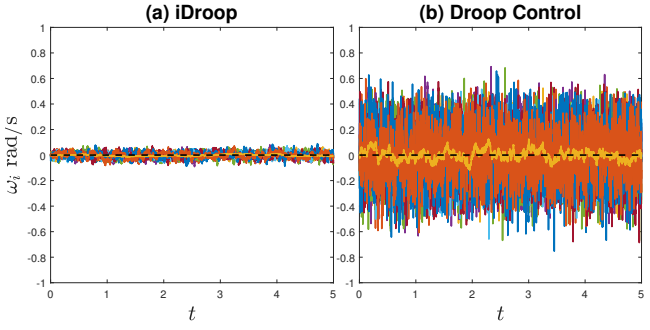

Fig. 4. Frequency deviations of the system when power disturbances and measurements noise are introduced with $k_p = 0.15$ and $k_\omega = 1.5$

The first simulation (figures 3 and 4) shows how iDroop and droop control perform when the system is subject to power disturbances and measurement noise. Figure 3 shows the frequency deviations of the system when $k_p = 1.5 \gg k_\omega = 0.15$, while Figure 4 shows the when $k_p = 0.15 \ll k_\omega = 1.5$. In both cases δ is set to be very low ($\delta = 0.001$), as required by the theory, and ν is set to be the optimal value $\nu^* = 9.75$ for $k_p \gg k_\omega$, and $\nu^* = 0.019$ for $k_p \ll k_\omega$. This shows that no matter which type of noise dominates, by choosing ν optimally and δ small enough, iDroop has better disturbance rejection than droop control.

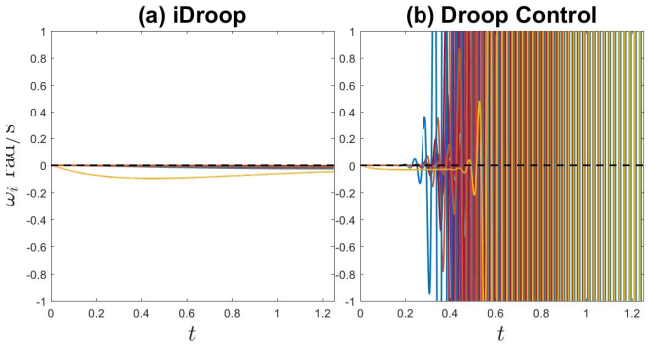

Fig. 5. Frequency deviations a delay $\tau = .02$ seconds is introduced in the frequency measurements

The second simulation shows how iDroop and droop control respond to delayed frequency measurements. Using $\delta = 0.001$, $R_{r,i} = 0.5$ and $\nu = 0.3$, our analysis shows that $\tau_{\text{rob}}^{\text{DC}} = 0.017$ for droop control, while for iDroop $\tau_{\text{rob}}^{\text{iDroop}} = 0.21$. The significant difference between the critical delays suggests that iDroop should be more robust to delays despite the heterogeneity. This is illustrated in Figure 5, which shows the frequency deviations of the system implementing iDroop and droop control with a frequency measurement delay of $\tau = 0.02$. It can be seen that iDroop is still able to stabilize the system in cases where droop control cannot.

VI. Conclusions and Future Works

This work aims to study the effect of using gird connected inverters to mitigate the dynamic degradation being experienced by the power grid. Our analysis shows that using dynamically controlled inverters like iDroop that drift away from the traditional virtual inertia and droop control mechanisms can provide a more efficient use of inverters that can further improve the power system performance in the presence of power disturbances and frequency noise, while providing larger robustness margins to delay. Future works include an extension of our analysis for heterogeneous system parameters as well as thorough experimental evaluation with more realistic network models.

References

[1] M. Milligan, B. Frew, B. Kirby, M. Schuerger, K. Clark, D. Lew, P. Denholm, B. Zavadil, M. O'Malley, and B. Tsuchida, "Alternatives No More Wind and Solar Power Are Mainstays of a Clean, Reliable, Affordable Grid," *IEEE Power and Energy Magazine*, vol. 13, no. 6, pp. 78–87, 2015.

[2] W. Winter, K. Elkington, and G. Bareux, "Pushing the Limits: Europe's New Grid: Innovative Tools to Combat Transmission Bottlenecks and Reduced Inertia," *IEEE Power and Energy Magazine*, 2015.

[3] North American Electric Reliability Corporation, "Eastern Interconnection Frequency Initiative Whitepaper," Dec. 2013.

[4] A. J. Wood, B. F. Wollenberg, and G. B. Sheble, "Power generation, operation and control," *John Wiley&Sons*, 1996.

[5] J. Boemer, K. Burges, C. Nabe, and M. Pöller, *All Island TSO Facilitation of Renewables Studies*. EirGrid and SONI, 2010.

[6] B. J. Kirby, "Frequency Regulation Basics and Trends," Oak Ridge National Laboratory, Tech. Rep., Jan. 2005.

[7] North American Electric Reliability Corporation, "Frequency Response Initiative Report," pp. 1–212, Oct. 2012.

[8] Federal Energy Regulatory Commission, "Essential Reliability Services and the Evolving Bulk-Power System—Primary Frequency Response ," Nov. 2016.

[9] J. Driesen and K. Visscher, "Virtual synchronous generators," in *IEEE Power and Energy Society General Meeting: Conversion and Delivery of Electrical Energy in the 21st Century, PES*. IEEE, New York, United States, Sep. 2008.

[10] E. Mallada, "iDroop: A dynamic droop controller to decouple power grid's steady-state and dynamic performance," in *55th IEEE Conference on Decision and Control (CDC)*, 2016.

[11] F. Paganini, Z. Wang, J. C. Doyle, and S. H. Low, "Congestion control for high performance, stability, and fairness in general networks," *IEEE/ACM Transactions on Networking*, vol. 13, no. 1, pp. 43–56, 2005.

[12] R. Pates and E. Mallada, "Decentralized robust inverter-based control in power systems," in *IFAC World Congress*, 2017.

[13] M. Ciobotaru, R. Teodorescu, and V. G. Agelidis, "Offset rejection for PLL based synchronization in grid-connected converters," in *Applied Power Electronics Conference and Exposition, 2008. APEC 2008. Twenty-Third Annual IEEE*. IEEE, 2008, pp. 1611–1617.

[14] F. Blaabjerg, R. Teodorescu, M. Liserre, and A. V. Timbus, "Overview of Control and Grid Synchronization for Distributed Power Generation Systems," *IEEE Transactions on Industrial Electronics*, vol. 53, no. 5, pp. 1398–1409, 2006.

[15] J. C. Doyle, K. Glover, P. P. Khargonekar, and B. A. Francis, "State-space solutions to standard H_2 and H_∞ control problems," *Automatic Control, IEEE Transactions on*, vol. 34, no. 8, pp. 831–847, Aug. 1989.

[16] E. Tegling, B. Bamieh, and D. F. Gayme, "The Price of Synchrony: Evaluating the Resistive Losses in Synchronizing Power Networks," *IEEE Transactions on Control of Network Systems*, vol. 2, no. 3, pp. 254–266, 2015.

[17] B. K. Poolla, S. Bolognani, and F. Dörfler, "Optimal Placement of Virtual Inertia in Power Grids," Oct. 2015.

[18] E. Tegling, M. Andreasson, J. W. Simpson-Porco, and H. Sandberg, "Improving performance of droop-controlled microgrids through distributed PI-control," Jan. 2016.

[19] Y. Jiang, R. Pates, and E. Mallada, "Performance tradeoffs of dynamically controlled grid-connected inverters in low inertia power systems," *arXiv preprint arXiv:1705.00547*, 2017.

[20] C. Desoer and Y. Wang, "On the generalized nyquist stability criterion," *IEEE Transactions on Automatic Control*, vol. 25, pp. 187–196, 1980.

[21] J. H. Chow and K. W. Cheung, "A toolbox for power system dynamics and control engineering education and research," *IEEE Transactions on Power Systems*, vol. 7, no. 4, pp. 1559–1564, 1992.